

Autonomous Loading of a Washing Machine with a Single-arm Robot

Hassan Shehawy^a, Andrea Maria Zanchettin^b and Paolo Rocco^c

Politecnico di Milano, 20133 Milan, Italy

Keywords: Robotics, Deformable Objects, Image Clustering, Computer Vision.

Abstract: The perception and autonomous manipulation of clothes by robots is an ongoing research topic that is attracting a lot of contributions. We consider the application of handling garments for laundry in this work. A framework for loading a washing machine with clothes placed initially inside a box is presented. Our framework is created in a modular way to account for the sub-problems associated with the full process. We extend our grasping point estimation algorithm by finding multiple grasping points and defining a score to select one. Active contours segmentation is added to the algorithm as well for more robust clustering of the image. Model of the washing machine is used to create a motion plan for the robot to place the clothes inside the drum. A new module is added for detection of items fallen outside the drum so to plan corresponding corrective action. We use ROS, depth and 2D cameras and the Doosan A0509 robot for experiments.

1 INTRODUCTION

Robots have been used in many projects with clothes for some time now and several works have been published with a wide variety of applications. For example in (Yamazaki et al., 2010), a robot was used for tidying a room which included manipulation of clothes whereas in (Yamazaki et al., 2014) the authors used a robot for assistance in dressing. The variation is not only in the application, but also the configuration of the system. If folding clothes is considered as an application, then a dual-arm robot was used in (Stria et al., 2014) while a single-arm one was used in (Petrík et al., 2017). Using various approaches for the perception is also noticeable which included the recognition of clothes and/or their state. Computer vision was used in many works either using a 2D camera as in (Yamazaki et al., 2011) or a depth camera as in (Sun et al., 2018). Haptics was also used as in (Clegg et al., 2017) and hybrid methods have been used as well in (Yuan et al., 2018) and (Kampouris et al., 2016).

Finding a grasping point is a fundamental step prior to the manipulation of clothes and different methods were used to detect one. In (Willimon et al., 2011b), a set of possible grasping points were calculated and an arbitrary one was selected while in other

works, features as wrinkles (Willimon et al., 2011a) and edges (Ramisa et al., 2011) were extracted. Modeling the grasping process was part of some works as in (Gil et al., 2016) and meanwhile some other works didn't consider it (Mira et al., 2015).

Even though there is a lot of works that have been published or ongoing, there are many open challenges to consider. In this paper, we present a full pipeline for loading a washing machine with clothes placed inside a laundry basket. We use a single-arm robot for the manipulation, 2D and an RGB-D camera for perception. Figure 1 shows the robot placing garments inside the washing machine.

To consider the full process of loading the washing machine, we created a modular approach that accounts for the different problems associated with the process. We extend our grasping point estimation algorithm (Shehawy et al., 2021) by finding curves in the image that can be bounding garments, possibly extracting multiple grasping points and defining thresholds for picking one. We use Active Contours for segmenting the image for more robust clustering. With the knowledge of the machine CAD model, a direction and a set of waypoints are used to create the motion plan for the loading process. Another module has been developed to detect if garments fall out of the drum and a corrective action is taken to put them back inside the drum. The contribution of this paper is the proposed framework which realizes the autonomous loading of a washing machine. It includes

^a <https://orcid.org/0000-0002-8369-8963>

^b <https://orcid.org/0000-0002-1866-7482>

^c <https://orcid.org/0000-0001-6716-434X>



Robot successfully grasped an item from a laundry basket and midway to place it inside the washing machine.

Figure 1: Robot loading clothes inside a washing machine.

our extended algorithm for finding a grasping point in a more robust way using active contours.

The paper is organized as follows. The next section explains the framework which includes finding a set of grasping points and selecting one according to predefined criteria, creation of motion plan, and checking the status of the loaded garments. Section 3 discusses the experiments and the practical aspects of the system which includes the design of the ROS nodes and the gripper.

2 METHOD

A dedicated framework for loading the washing machine has been developed and is presented in this section. The first part is finding a grasping point and to this, we focus on finding a continuous area in the image of the loaded basket and use its centroid as a grasping point. To account for the possible failures in the process, we add two modules for detecting and correcting such situations. The first one is checking if an item is partially outside the washing machine after being placed inside the drum. The second one is checking the floor to see if any item(s) has fallen during the process of loading the washing machine.

2.1 Grasping Point

In this work, Active Contours method is used for segmentation, and centroids of clusters (that identify different clothes) are all considered as grasping points. A set of weights is introduced for assessment of the points to select one. We use our SW-filter that we have presented in our previous work (Shehawey et al., 2021) before the segmentation.

2.1.1 Pre-segmentation

Prior to the segmentation, each pixel in position (x, y) is given the value:

$$I(x, y) = \sqrt{P_L L(x, y)^2 + P_a a^*(x, y)^2 + P_b b^*(x, y)^2}$$

where $L(x, y)$, $a^*(x, y)$ and $b^*(x, y)$ correspond to the conversion from the RGB to the La^*b^* (Ganesan et al., 2010) color space. P_L , P_a and P_b are parameters to allow for the balance of luminance and color weights for images. Results were very sensitive to the selection of these parameters, and they were set as $P_L = 4$, $P_a = 1.5$ and $P_b = 1.5$.

2.1.2 Clustering using Active Contours

Active Contours methods rely on the concept of an energy functional that is minimized to find a curve of interest inside an image (Kass et al., 1988). The functional is a combination of two components, one of them controls the smoothness of the curve and the other brings the curve closer to the boundary. The curve is assumed to form a contour around the objects in the image. It can be represented implicitly as

$$C = \{(x, y) | u(t, x, y) = 0\}$$

and its evolution can be described by the PDE:

$$\frac{\partial u}{\partial t} = F |\nabla u|$$

where F represents the speed of the evolution and may be chosen as the curvature. In this case, the PDE becomes:

$$\frac{\partial u}{\partial t} = \text{div} \left(\frac{\nabla u}{|\nabla u|} \right) |\nabla u|$$

where $\text{div} \left(\frac{\nabla u}{|\nabla u|} \right)$ stands for the divergence of the normalized gradient which is the curvature calculated on the level-sets of u .

This approach has been extended in multiple works like the the Active Contours Without Edges (ACWE) (Chan and Vese, 2001) and the Geodesic Active Contours (GAC) (Caselles et al., 1995). We use the GAC method here where the curve evolution

based on the energy functional introduced in (Caselles et al., 1995) is defined as:

$$\frac{\partial u}{\partial t} = g(I)|\nabla u| \operatorname{div}\left(\frac{\nabla u}{|\nabla u|}\right) + \nabla u \nabla g(I)$$

where $g(I)$ is the function that dictates the regions of interest in the image and it is usually selected to highlight the edges in the image. In our work we used this form:

$$g(I) = \frac{1}{\sqrt{1 + \alpha|\nabla \hat{I}|}}$$

where \hat{I} is a smoothed image obtained by applying a Gaussian filter (with standard deviation σ) on the image I and α is an empirical parameter.

To overcome the problems associated with a wrong initial guessed curve u_0 or the curve passing through noisy points that can stop the curve evolution, the balloon force is added to the functional as described in (Cohen, 1991) and hence the curve evolution becomes:

$$\frac{\partial u}{\partial t} = g(I)|\nabla u| \operatorname{div}\left(\frac{\nabla u}{|\nabla u|}\right) + \nabla u \nabla g(I) + |\nabla u|g(I)\nu$$

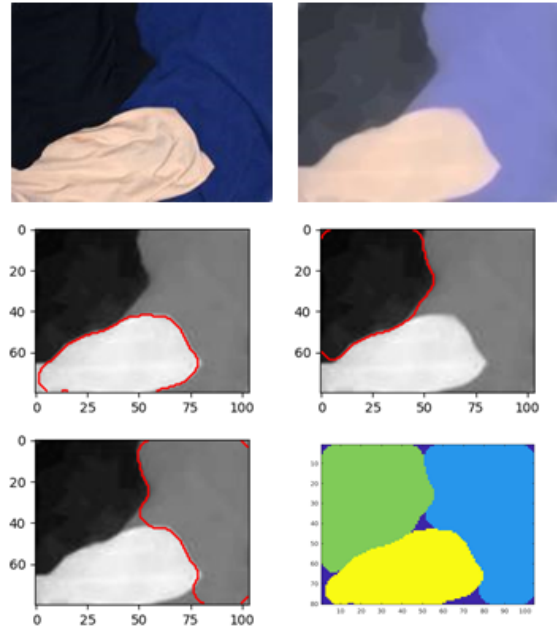
where $\nu \in \mathbb{R}$ is the parameter for the balloon force.

Replacing differential operators with morphological ones helps in decreasing the numerical and computational complexity associated with solving PDEs as introduced in (Marquez-Neila et al., 2014) which presents a full framework for implementing the ACWE and GAC using morphological operations. To reduce the time associated with this step, we adopt this technique of implementing the GAC method.

2.1.3 Post-segmenting

An initial level set of a circle with a small radius was used and running the segmentation with that initial curve at different points could cluster the different garments in the image. These clusters can be combined together into one segmented image as shown in Figure 2 where three garments are successfully segmented. To complete the segmentation step and address some possible problems, we perform this extra step: for every pair of clusters (C_i and C_j), the intersection ($C_{ij} = C_i \cap C_j$) is calculated and a ratio η is defined as an intersection threshold (set at 0.95). Then the number of elements in the clusters and their intersection is computed and:

- if $n(C_{ij})/n(C_i) > \eta$ and $n(C_{ij})/n(C_j) > \eta$, they are combined into one cluster.
- if $n(C_{ij})/n(C_i) > \eta$ and $n(C_{ij})/n(C_j) < \eta$, the median values of the clusters are computed. If the difference between them is small, the two clusters



Input image of clothes (left) and the result of applying our SW-filter (right) are in first row. Running MGAC clustering at different points gave the results in second and third (left) rows while the combination of the clusters is shown in the third row (right).

Figure 2: Image Clustering using MGAC.

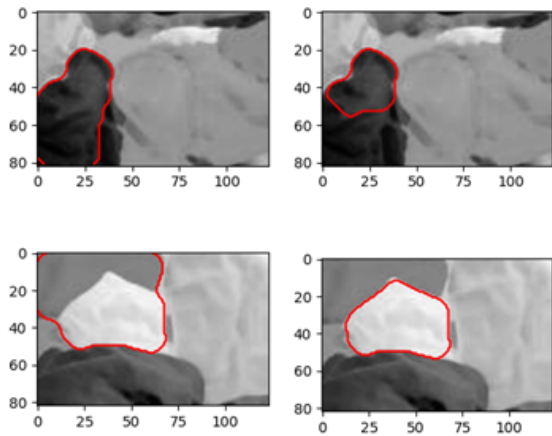
are combined into one. An example of this case is shown in Figure 3 (upper row). Otherwise, we have two clusters; one of them is the smaller cluster and the other is the difference between the two clusters. An example of this case is shown in Figure 3 (lower row).

2.1.4 Weights of Grasping Points

The main criterion for selecting a grasping point is the area of the cluster. However, two more criteria are added to consider other factors in selecting the point:

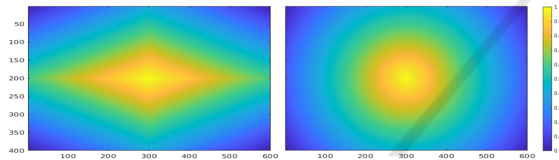
- Normal distances from the horizontal and vertical edges, w_{eh} and w_{ev} . These weights are corrected by scaling the distance to the longer edge by a factor (we chose it as the ratio of the longer to the smaller edge). This is illustrated in Figure 4 (on the left).
- Euclidean distance from the center of the basket, w_{rc} . We consider the reciprocal of the distance as a weight so that the closer the point to the center, the higher the weight. This is illustrated in Figure 4 (on the right).

The final weight is the sum of the normalized weights w_{rc} , w_{eh} and w_{ev} . The detected clusters are sorted according to their area and the largest one is considered for grasping. However, if multiple clusters have an



Two examples of intersection of two clusters where analysis is needed. In upper row, the smaller cluster (right) is indeed part of the bigger one (left). In the lower row, this is not the case and it is an independent cluster.

Figure 3: MGAC Segmentation Intersection.



Distance from the edges (left) is one criterion for a grasping point while distance from the center (right) is another one.

Figure 4: Weights of Grasping Points.

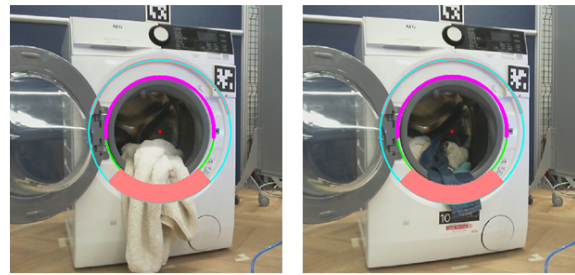
area $> 40 \text{ cm}^2$, we use the weight defined here to select a point.

2.2 Checking for Items Partly Outside the Drum

The first inspection is to check if the loading process was indeed successful in terms of placing the item completely inside the drum and making sure that no part of it is still outside the drum. For this we detect the drum opening by finding two circles in the image using Hough Transform (Yuen et al., 1990). To ensure that the correct circle is detected, we place a fiduciary marker (AprilTag (Wang and Olson, 2016)) at a known position relative to the drum center. A region of interest (ROI) is created as the disk between the smaller and larger circle. Figure 5 shows two examples for this process where the two circles and the disk of interest are highlighted.

To check this region, we convert the image from the Cartesian space into the log-polar one. This is done using the following equation:

$$\rho = \log(\sqrt{(x - x_c)^2 + (y - y_c)^2})$$



Region Of Interest (ROI) is created to check if an item is partially outside the washing machine. Two examples are shown here with a dark color (right) and a more challenging bright color (left).

Figure 5: Inspection of the outer part of the drum.

and

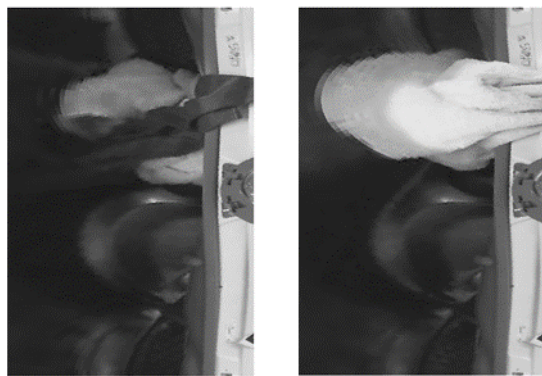
$$\theta = \tan^{-1} \frac{y - y_c}{x - x_c}$$

where x_c and y_c are the center coordinates in the Cartesian space. In the new space, the curved area of interest is now a rectangular patch in the image. This requires the correct positioning of the center of the transformation which is set as the center of the drum. Figure 6 (a) shows the output of this transformation applied to the images in Figure 5.

Prior to the loading process, an image I_{od} is captured for the washing machine when the drum is empty and used as a reference to compare against it. For a new image I , the difference $|I - I_{od}|$ is calculated and in this difference image pixels with values less than a threshold (set at 50) are ignored. Figure 6 (b) shows the ROI and difference images for the setup in Figure 5.

2.3 Checking for Items Fallen on the Floor

We use the same idea here as well by having an image I_{of} for the floor before the loading process. However, here we find the difference for a new image I $|I - I_{of}|$, using the HSV (Sural et al., 2002) color space. To adjust for the possible variations of the garments colors, we calculate the difference in the hue and value channels of the HSV. In some cases, the difference in the hue channel is very small and will not lead to identification of fallen items. In other cases, this can happen in the value channel as well and therefore, we consider the larger value. Figure 7 shows an example for two items where the hue difference gave better results in one case and the value difference showed better results in the other one. We apply morphological closing on the difference image and then find the largest connected component that represents the item on the floor as shown in Figure 7.



(a)



(b)

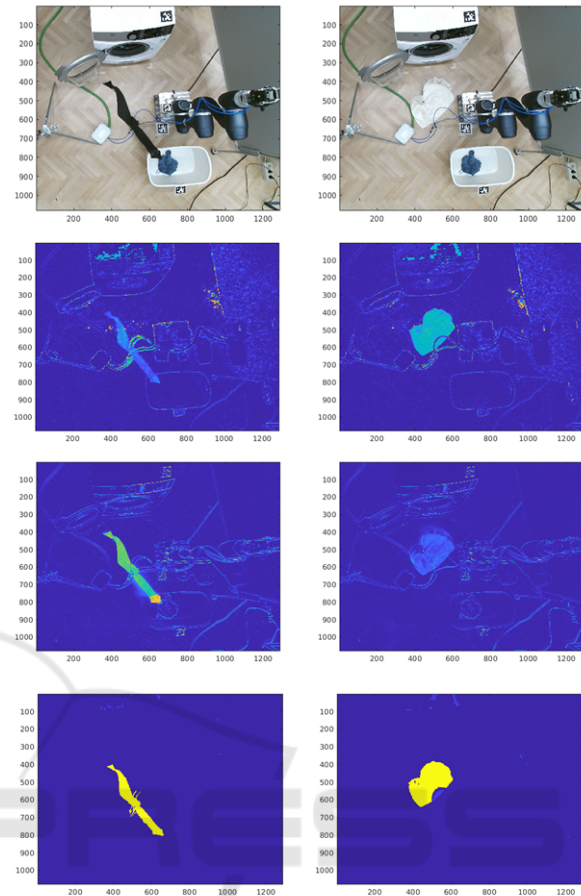
Images from Figure 5 are transformed to log-polar space in (a). In (b), both the ROI and difference images are shown. ROI image is the disk between the inner and outer circle of the drum. Difference image is obtained based on an initial image taken before the loading process. For dark objects, detection is easier because the contrast against the white surface is higher (as in upper two images). For bright ones, it is more challenging as the contrast is lower. However, the wrinkles are helpful in recognizing the garment (as in lower two images).

Figure 6: Analyzing the drum images.

2.4 Planning Robot Movements

For an efficient grasping, fingers need to create some wrinkles/creases when they close. This is more probable and effective when the gripper reaches the clothes vertically. To do this we define a point that is shifted upwards from the grasping point by 10 cm and move the arm from it to the grasping point. After the gripper closes, the arm will not move immediately to the washing machine, but above the basket so that a grasped item would fall inside the basket if it slips.

When the arm is placing an item inside the drum, a path is designed to make the robot push down the clothes already within the drum in a coherent way.



Images of the floor captured after the loading process to check for any fallen item(s). Raw images are shown in the first row. The second and third rows show the difference with images of floor before the loading process in the hue channel of the HSV and the saturation channel. Fourth row show the extraction of the largest component that corresponds to the fallen garment.

Figure 7: Floor Inspection.

With the washing machine CAD model, locating the drum center can be done using an AprilTag with known position relative to the washing machine. Figure 8 (left) shows the washing machine model, the drum axis and the AprilTag. A point is defined with respect to the drum center as a pre-entry point for the robot. Figure 8 (middle) shows this point. The path is generated from that point to the drum taking into consideration collision avoidance with the drum. Figure 8 (right) shows the robot inside the drum.

If an item is detected as partially outside the drum, the robot moves to the detected item, grasps it and then moves up towards the drum center and then inside it. Figure 9 shows an example of a sequence of placing an item back into the drum.



The detection of the AprilTag placed on top of the washing machine allows for finding the location of the center of the drum with the knowledge of the washing machine CAD model. The direction of the AprilTag x-axis (in red) also dictates the direction of the drum central axis (left). The actual pre-entry point (middle) and inside the drum one (right) are shown for the robot with the grasped item.

Figure 8: Washing Machine Drum Axis.



After checking if there's partial fall on the drum, the robot moves item into the drum.

Figure 9: Robot moving item inside the drum.

3 EXPERIMENTS

We use the Doosan A0509 collaborative robot, Kinect V2 depth camera and Microsoft LifeCam camera. Figure 10 shows the system components which is the used setup in our simulation environment. For implementing the framework, we used ROS (Quigley et al., 2009) Melodic and the PCL library (Rusu and Cousins, 2011) for handling the point cloud captured



All system components (including washing machine, laundry basket, the robot and the cameras) in the simulation inside rviz.

Figure 10: Simulation Setup.

from the Kinect camera. The generation of trajectories was done using MoveIt (Coleman et al., 2014) and for execution, it was communicated to the Doosan motion controller. The dimensions of the laundry basket and the CAD model of the washing machine are assumed to be known. This information was included into our URDF model but the location and orientation of them can be adjusted based on the AprilTag attached to the basket and the washing machine.

Clothes were randomly thrown into the basket and the robot could successfully grasp the items and place them inside the drum. We had 8 garments in total varying in size, color and texture. They were put in random configurations 5 times and the loading pipeline was tested. We had 34 loading attempts where a loading attempt is defined as a complete execution of the pipeline starting from identifying a grasping point and ending by releasing the garment inside the drum. Out of the 34 loading attempts we had:

- 18 completely successfully attempts. Complete success is defined as placing the garment completely inside the drum
- 11 partially successfully attempts. Partial success is defined as placing the garment inside the drum while part of it is partially outside the drum.
- 5 failed attempts. Failed attempt corresponds to

the cases when garments fall on the floor.

The partially successfully and failed attempts cases were mostly related to the large items like trousers or big towels. However, with the two modules for checking the drum and the floor, the garments could be placed inside the drum.

We created two ROS packages; one for the perception and the other for planning and executing the movements. The perception package included the following nodes:

- ROI-Creation Nodes: extracting the clothes inside laundry basket and the drum opening. These nodes published the cropped images.
- Inspection Nodes: checking the drum if an item is out and another for checking the floor. These nodes publish a boolean message (there is an item to grasp or not).
- Grasping-Points Nodes: finding a grasping point in the laundry basket, on the drum edge and on the floor (if items were detected). These nodes publish a 3D point in the end-effector frame.

The planning package included the following nodes:

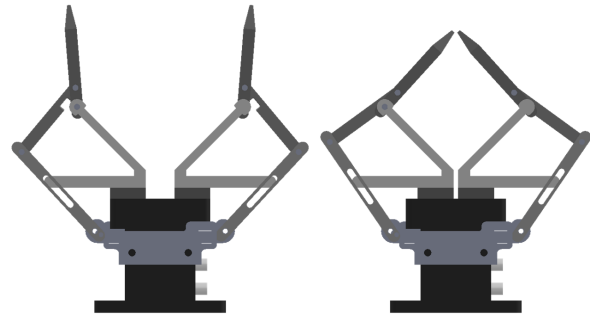
- Loading Node: it subscribes to the grasping point message and creates a motion plan for grasping clothes, moving upwards above the basket and then into the drum passing by the pre-entry point.
- Corrections Nodes: they subscribe to the inspection nodes boolean messages. If a correction is needed, they move the robot to a grasping point and either puts the partially-out item back into drum or the fallen item on the floor into the washing machine.

We use the Camozzi CGPS pneumatic gripper for grasping the clothes. However, the maximum aperture is very small (2 cm) does not give satisfactory results as it only works with clothes of small sizes and rough surfaces when there is enough friction force. But for the general case, wrinkles have to be formed inside the gripper to get a reliable grasping. To do this, we designed the gripper shown in Figure 11 that uses linkages for converting linear motion to rotary one and thus extends the maximum aperture.

A demonstration for the loading sequence and recovery modules can be viewed here: <https://www.youtube.com/watch?v=rK4GwbaqT8Q>

4 CONCLUSIONS

Using our proposed framework it was possible to autonomously load a washing machine with clothes placed inside a basket. Our framework is modular



Fingers attached to the pneumatic gripper with this mechanism created better grasping and grip .

Figure 11: Gripper in open/close positions.

in its design to allow for the recovery of failures, when needed. Active Contours showed robust clustering of the image without prior knowledge of the number or colors of items in the basket or even an estimate number of it. Despite the incomplete clustering of the image in some cases, clusters were created and a grasping point was found. More complete clustering could be achieved by adding more points for the initial curve. However this would add to the runtime and complexity of the work and such a complete clustering of the image is not needed as the main objective is to find at least one continuous area to consider for grasping which could be achieved using fewer number of points. The grasped item(s) could be placed inside the drum and when this failed, the recovery modules for drum and floor checking ensured the completion of the loading. Most of the failures were associated with big or heavy items that either slipped from the robot or were not completely placed inside the drum. A deeper grasp could be achieved by shifting the grasping point downwards by a few centimeters. This resulted in more success by having a firm grip but also increased the probability of grasping other item(s) that could be below it which could result in falling the items on the ground. Again, this kind of failure could be recovered by our floor inspection module.

Possible extensions for this work can rely on machine learning to detect a grasping point and use Dynamical Movement Primitives (DMP) to learn a trajectory for the loading process. Multi-fingers gripper can also be utilized for more robust and firm grasping.

REFERENCES

- Caselles, V., Kimmel, R., and Sapiro, G. (1995). Geodesic active contours. In *IEEE International Conference on Computer Vision*, pages 694—699.

- Chan, T. and Vese, L. (2001). Active contours without edges. *IEEE Transactions on Image Processing*, 10(2), pages 266—277.
- Clegg, A., Yu, W., Erickson, Z., Tan, J., Liu, C., and Turk, G. (2017). Learning to navigate cloth using haptics. In *IEEE International Conference on Intelligent Robots and Systems*, pages 2799–2805. Institute of Electrical and Electronics Engineers Inc.
- Cohen, L. D. (1991). On active contour models and balloons. *CVGIP: Image Understanding*, vol. 53, no. 2, pages 211–218.
- Coleman, D., Sucas, I., Chitta, S., and Correll, N. (2014). Reducing the barrier to entry of complex robotic software: a moveit! case study. pages 1–14.
- Ganesan, P., Rajini, V., and Rajkumar, R. (2010). Segmentation and edge detection of color images using cielab color space and edge detectors. In *International Conference on "Emerging Trends in Robotics and Communication Technologies"*, INTERACT-2010. IEEE.
- Gil, P., Mateo, C. M., Delgado, Á., and Torres, F. (2016). Visual/Tactile sensing to monitor grasps with robot-hand for planar elastic objects. *47th International Symposium on Robotics, ISR 2016*, 2016:439–445.
- Kampouris, C., Mariolis, I., Peleka, G., E. Skartados, E., Kargakos, A., Triantafyllou, D., and Malassiotis, S. (2016). Multi-sensorial and explorative recognition of garments and their material properties in unconstrained environment. In *IEEE International Conference on Robotics and Automation (ICRA)*, pages 1656–1663. IEEE.
- Kass, M., Witkin, A., and Terzopoulos, D. (1988). Snakes: Active contour models. *International Journal of Computer Vision*, 1(4), pages 321—331.
- Marquez-Neila, P., Baumela, L., and Alvarez, L. (2014). A morphological approach to curvature-based evolution of curves and surfaces. In *IEEE Transactions on Pattern Analysis and Machine Intelligence*, 36(1), pages 2—17.
- Mira, D., Delgado, A., Mateo, C. M., Puente, S. T., Candelas, F. A., and Torres, F. (2015). Study of dexterous robotic grasping for deformable objects manipulation. *2015 23rd Mediterranean Conference on Control and Automation, MED 2015 - Conference Proceedings*, pages 262–266.
- Petrik, V., Smutný, V., Krsek, P., and Hlaváč, V. (2017). Single arm robotic garment folding path generation. *Advanced Robotics*, 31(23-24):1325–1337.
- Quigley, M., Gerkey, B., Conley, K., Faust, J., Foote, T., Leibs, J., Berger, E., Wheeler, R., and Ng, A. (2009). Ros: an open-source robot operating system. In *IEEE Intl. Conf. on Robotics and Automation (ICRA) Workshop on Open Source Robotics*.
- Ramisa, A., Alenya, G., Moreno-Noguer, F., and Torras, C. (2011). Determining where to grasp cloth using depth information. *Frontiers in Artificial Intelligence and Applications*, 232:199–207.
- Rusu, R. B. and Cousins, S. (2011). 3d is here: Point cloud library (pcl). In *IEEE International Conference on Robotics and Automation*, pages 19–22.
- Shehawy, H., Rocco, P., and Zanchettin, A. (2021). Estimating a garment grasping point for robot. In *20th International Conference on Advanced Robotics (ICAR)*. IEEE.
- Stria, J., Prusa, D., Hlavac, V., Wagner, L., Petrik, V., Krsek, P., and Smutny, V. (2014). Garment perception and its folding using a dual-arm robot. *IEEE International Conference on Intelligent Robots and Systems*, (September):61–67.
- Sun, L., Aragon-Camarasa, G., Rogers, S., and Siebert, J. P. (2018). Autonomous Clothes Manipulation Using a Hierarchical Vision Architecture. *IEEE Access*, 6(October):76646–76662.
- Sural, S., Qian, G., and Pramanik, S. (2002). Segmentation and histogram generation using the hsv color space for image retrieval. In *IEEE International Conference on Image Processing*, pages 589–592.
- Wang, J. and Olson, E. (2016). Apriltag 2: Efficient and robust fiducial detection. In *IEEE International Conference on Intelligent Robots and Systems*, pages 4193—4198.
- Willimon, B., Birchfield, S., and Walker, I. (2011a). Classification of clothing using interactive perception. In *IEEE International Conference on Robotics and Automation*, pages 1862–1868.
- Willimon, B., Birchfield, S., and Walker, I. (2011b). Model for unfolding laundry using interactive perception. In *IEEE International Conference on Intelligent Robots and Systems*, pages 4871–4876. IEEE.
- Yamazaki, K., Nagahama, K., and Inaba, M. (2011). Daily clothes observation from visible surfaces based on wrinkle and cloth-overlap detection. *Proceedings of the 12th IAPR Conference on Machine Vision Applications, MVA 2011*, pages 275–278.
- Yamazaki, K., Oya, R., Nagahama, K., Okada, K., and Inaba, M. (2014). Bottom dressing by a life-sized humanoid robot provided failure detection and recovery functions. *2014 IEEE/SICE International Symposium on System Integration, SII 2014*, pages 564–570.
- Yamazaki, K., Ueda, R., Nozawa, S., Mori, Y., Maki, T., Hatao, N., Okada, K., and Inaba, M. (2010). System integration of a daily assistive robot and its application to tidying and cleaning rooms. *IEEE/RSJ 2010 International Conference on Intelligent Robots and Systems, IROS 2010 - Conference Proceedings*, pages 1365–1371.
- Yuan, W., Mo, Y., Wang, S., and Adelson, E. H. (2018). Active clothing material perception using tactile sensing and deep learning. In *IEEE International Conference on Robotics and Automation (ICRA)*, pages 4842–4849. IEEE.
- Yuen, H., Princen, J., Illingworth, J., and Kittler, J. (1990). Comparative study of hough transform methods for circle finding. *Image and Vision Computing*, 8(1):7177.